Development 130, 3095-3109

doi:10.1242/dev.00530

Loss of Bmp7 and Fgf8 signaling in Hoxa13-mutant mice causes hypospadia

Emily A. Morgan[2], Susan B. Nguyen[1], Virginia Scott[1] and H. Scott Stadler[1,2,*]

[1]Shriners Hospital for Children, Portland, OR 97239, USA
[2]Oregon Health and Sciences University, Department of Molecular and Medical Genetics, 3181 SW Sam Jackson Park Road, Portland, OR 97239, USA
*Author for correspondence (e-mail: hss@shcc.org)

Accepted 8 April 2003

SUMMARY

In humans and mice, mutations in *Hoxa13* cause malformation of limb and genitourinary (GU) regions. In males, one of the most common GU malformations associated with loss of *Hoxa13* function is hypospadia, a condition defined by the poor growth and closure of the urethra and glans penis. By examining early signaling in the developing mouse genital tubercle, we show that *Hoxa13* is essential for normal expression of *Fgf8* and *Bmp7* in the urethral plate epithelium. In *Hoxa13*^{GFP}-mutant mice, hypospadias occur as a result of the combined loss of *Fgf8* and *Bmp7* expression in the urethral plate epithelium, as well as the ectopic expression of noggin (*Nog*) in the flanking mesenchyme. In vitro supplementation with Fgf8 restored proliferation in homozygous mutants to wild-type levels, suggesting that *Fgf8* is sufficient to direct early proliferation of the developing genital tubercle. However, the closure defects of the distal urethra and glans can be attributed to a loss of apoptosis in the urethra, which is consistent with reduced *Bmp7* expression in this region. Mice mutant for *Hoxa13* also exhibit changes in androgen receptor expression, providing a developmental link between *Hoxa13*-associated hypospadias and those produced by antagonists to androgen signaling. Finally, a novel role for *Hoxa13* in the vascularization of the glans penis is also identified.

Key words: *Hoxa13*, Mouse, Genitourinary development, Hypospadia

INTRODUCTION

In humans and mice, reproduction occurs by internal fertilization, a strategy facilitated by the formation of specialized external genitalia. Developmentally, these structures are derived from the genital tubercle (GT), a ventro-caudal structure composed of bilateral shelves of mesenchyme bisected by a central epithelial plate (Cunha, 1972; Murakami, 1987; Kurzrock et al., 1999). At approximately 50 days of human gestation (embryonic day 14-15 in mice), the sexually ambiguous genitalia begin to exhibit secondary sexual characteristics, a process initially believed to be mediated solely by the presence (male) or absence (female) of androgen signaling (Cunha and Lung, 1978; Murakami, 1987; Murakami and Mizuno, 1986).

Recently, new evidence suggests that androgens are not the sole regulators of GT patterning. In particular, many genes whose proteins provide the instructive signals necessary for limb development also play a predominant role during GT formation, including members of the fibroblast growth factor (*Fgf8* and *Fgf10*), hedgehog (*Shh*) and Hox (*Hoxa13* and *Hoxd13*) gene families (Haraguchi et al., 2000; Haraguchi et al., 2001; Stadler et al., 2001; Zhao and Potter, 2001; Warot et al., 1997; Mortlock and Innis, 1997; Podalesk et al., 1997; Podalesk et al., 1999; van der Hoeven et al., 1996a; van der Hoeven et al., 1996b). Finally, human androgen receptor mutations are generally rare in individuals exhibiting some of the more common genitourinary (GU) malformations such as hypospadia, a condition characterized by arrested growth, formation and closure of the external genitalia (Sutherland et al., 1996; Allera et al., 1995). In males, hypospadia can affect several different regions of the developing glans penis. These malformations range from distal defects, impacting the placement and formation of the urethral opening or meatus (coronal hypospadia), to more proximal defects, affecting the growth and closure of the ventral urethra (penile hypospadia), scrotum (scrotal hypospadia) and peritoneum (peritoneal hypospadia) (Baskin, 2000; Silver and Russel, 1999; Sutherland et al., 1996; Allera et al., 1995).

To date, little is known about the cellular and molecular mechanisms underlying this malformation; however, the incidence of hypospadia appears to be increasing dramatically, affecting as many as 1 in 125 live male births each year (Baskin et al., 1998; Baskin et al., 2001; Gallentine et al., 2001; Paulozzi et al., 1997). Recently, mutations in the transcription factor *Hoxa13* were shown to cause Hand-Foot-Genital Syndrome (HFGS), an autosomal dominant disorder that profoundly affects the development of many genitourinary structures, including the uterus, bladder, ureters and cervix, as well as causing hypospadia (Stern et al., 1970; Pozanski et al., 1975; Giedion and Prader, 1976; Mortlock and Innis, 1997; Goodman et al., 2000).

Using gene targeting in mice, similar mutations that phenocopy HFGS (Stadler et al., 2001; Fromental-Ramain,

1996; Warot et al., 1997) have been generated. From these initial studies, a role for *Hoxa13* in patterning both limb and caudal GU structures has been established. In particular, mice lacking *Hoxa13* exhibited gross malformations of the rectum, Müllerian ducts, ureters and bladder (Warot et al., 1997).

Recognizing both the increasing frequency of hypospadia in the human population, as well as its association with HFGS, we hypothesized that many of the cellular and molecular mechanisms underlying this malformation could be identified in *Hoxa13*-mutant mice. In this report, we present evidence that mice mutant for *Hoxa13* phenocopy the hypospadia in HFGS, causing malformation of the distal glans and meatus, as well as closure defects of the ventral urethra. At the molecular level, we demonstrate that *Hoxa13* function is essential for the normal expression of *Fgf8* and *Bmp7* in the developing urethral epithelium, as well as for the repression of noggin (*Nog*) expression in the mesenchyme flanking the urethral plate epithelium (UPE). Next, we demonstrate that supplementation with Fgf8 in the urethral epithelium is sufficient to restore proliferation in the developing GT. Furthermore, we show that *Bmp7* provides an apoptotic signal to the UPE and flanking mesenchyme, as antibody blocking of *Bmp7* is sufficient to reduce most programmed cell death (PCD) in these regions. Interestingly, the blocking of either *Bmp4* or *Bmp7* signaling during GT outgrowth recapitulated many of the defects exhibited by *Hoxa13*^{GFP} homozygous mutant mice, confirming that perturbations in Bmp signaling contribute to the coronal and penile hypospadias exhibited by these mice. Finally, a novel role for *Hoxa13* in mediating the vascularization of the glans penis was also identified during this study.

MATERIALS AND METHODS

Hoxa13^{GFP} mice

The *Hoxa13*^{GFP} allele originally described by Stadler et al. (Stadler et al., 2001) was utilized in all experimental procedures. Heterozygous intercrosses were utilized to produce both homozygous *Hoxa13*^{GFP}-mutant (–/–) and wild-type (+/+) embryos. Examination of the developing genitourinary regions revealed no differences between heterozygous mutant and wild-type embryos with respect to growth, morphology and gene expression patterns. Gestational ages were defined as embryonic days (E), where the detection of a vaginal plug denotes E 0.5. Embryo genotypes were determined by PCR using yolk sac-derived DNA and primers as described previously (Stadler et al., 2001). Embryonic sex was determined by PCR of yolk sac DNA with forward (5′-GAGAGCATGGAGGGCCAT-3′) and reverse (3′-CCACTCCTCTGTGACACT-5′) primers specific for murine *Sry*. All care and analysis of *Hoxa13*^{GFP} mice was carried out in accordance with an approved mouse handling protocol.

Fluorescent imaging

GFP, CY5 or Texas-Red fluorescence was assessed using a Bio-Rad MRC 1024 confocal imaging system fitted with a Leica DMRB microscope, using filter sets provided by the manufacturer. Whole-mount images represent 150 to 200 μm z-series stepped at 2 μm intervals, whereas cryosections were imaged in single planes using the GFP-tagged nucleus as the primary focal plane. A Kalman digital averaging filter was used to reduce random noise.

Immunohistochemistry

Primary antibodies used were Cytokeratin 14 (#RDIMCYTOK14abr, Research Diagnostics), Cytokeratin 5 (#RDIMCYTOK5abr, Research Diagnostics), Cytokeratin 8/18 (#RDI-Progp11, Research Diagnostics), anti-phosphohistone H3 (#06-570, Upstate Biotechnology), Pecam (CD31; #550274 BD, PharMingen).

Whole-mount analysis

E11.5-15.5 male embryos were fixed for 1 hour in 4% paraformaldehyde/1×phosphate buffered saline (PBS) at 4°C. The fixed tissues were rinsed four times (for 5 minutes each time) in 1×PBS, and then blocked in PBS containing 1% Triton X-100 (PBX), 2% skimmed milk and 5% donkey serum. Primary antibodies were incubated with the blocked tissues at 4°C overnight using previously determined concentrations. Embryos were then rinsed in 1×PBX, 2% skimmed milk for 3 hours at room temperature, followed by overnight incubation with either Texas-Red or CY5-conjugated secondary antibodies (Jackson Immuno Research) in PBX, 2% skimmed milk, 5% donkey serum at 4°C.

Cryosection analysis

Embryos were fixed as described above, followed by a 30 minute rinse in 1×PBS. Cryoprotection of the tissues was achieved using a sequential series of 10-40% sucrose/1×PBS. The embryos were oriented in OCT (Tissue-Tek) and frozen rapidly on dry ice. The embryos were sectioned to 15 μm using a Leitz Kryostat 1740, and mounted on Superfrost plus slides (Fisher) for analysis. Sections were rinsed for 10 minutes three times in 1×PBS to remove the OCT. Next the sections were permeabilized and blocked for 1 hour in PBX, 2% skimmed milk, 5% donkey serum. After blocking, primary antibodies were incubated on the sections for either 1 hour at room temperature or overnight at 4°C, using the same blocking solutions at previously determined concentrations. The sections were then rinsed in 1×PBX, 2% skimmed milk for 2 hours. Species-specific secondary antibodies conjugated with either Texas-Red or CY5 fluorochromes (Jackson Immuno Research) were incubated with the sections overnight at 4°C.

RNA in situ hybridization

Antisense riboprobes specific for *Bmp4*, *Bmp7*, *Msx1*, gremlin (*Cktsf1b1* – Mouse Genome Informatics) and *Fgf8* were generated using plasmids kindly provided by B. Hogan (*Bmp4*), R. Beddington (*Bmp7*), Y. Chen (*Msx1*), R. Harland (gremlin) and A. Moon (*Fgf8*). *Hoxa13*, *Shh*, *Bmpr1a*, *Bmpr1b*, *Bmpr2* and *Msx2* riboprobes were produced using PCR amplifications of gene-specific exons. The amplifying primers were:

Hoxa13, 5′-GCTGCCCTACGGCTACTTC-3′ and 5′-CAGGGCTGATAGCTTTCCAT-3′;

Shh, 5′-GCGCTCTTTGCCAGCCGCGT-3′ and 5′-TCAGCTGGACTTGACCGCCATT-3′;

Bmpr1a, 5′-CTGCATCAAGACTCCAATCCT-3′ and 5′-ACATGGAGTTTGGCCTTCAC-3′;

Bmpr1b, 5′-TGCAGATATCAAAGGGACTGG-3′ and 5′-AAGCCCAGGTCTGCTATGCA-3′;

Bmpr2, 5′-GACTTCACACAGGCTGCAAA-3′ and 5′-AAACGATCCAGAACCCCTTC-3′; and

Msx2, 5′-TCAGTCTGCCCTTCCCTA-3′ and 5′-ATATAAAAAGTCTTATATTTTATTAT-3′.

Amplified exons were cloned into a t-tailed vector containing RNA polymerase T3 and T7 promoters. Embryo preparation, hybridization and analysis was performed as described by Manley and Capecchi (Manley and Capecchi, 1995).

TUNEL analysis of apoptosis

TUNEL analysis was performed as described by Stadler et al. (Stadler et al., 2001). Genital tubercles from E12.5 heterozygous- and homozygous-mutant embryos were examined by confocal analysis of 200 μm *z*-series as described above. TUNEL analysis on frozen sections followed the same approach as whole-mount TUNEL assays using 20 μm sections through the genital tubercle.

Organ culture with Fgf8b and DHT supplementation

Heparin acrylic beads (#H-5263, Sigma), containing either 0.1 mg/ml BSA (control) or 0.1mg/ml Fgf8b (R and D Systems), were placed in the UPE of E11.5 male embryos. Tissue explants containing the bead-implanted genital tubercles were placed on cellulose membranes supported by stainless steel mesh in 60 mm organ culture dishes containing BGJb media (Sigma-Aldrich), supplemented with 50 U/ml penicillin, 25 μg/ml streptomycin and 0.1 mg/ml ascorbic acid, and grown for 24 hours in a incubator at 37°C containing air supplemented with 5% CO_2. The GT explants were examined for changes in cell proliferation using the anti-phosphohistone-H3 antibody (Upstate Biotechnology).

Extended growth response of the GT to Fgf8b was performed using BGJb media, supplemented with 0.1 mg/ml Fgf8b or BSA, in a BTC Engineering rotary culture apparatus. E11.5 GTs were dissected from *Hoxa13*^{GFP} heterozygous and homozygous mutant embryos and grown for 72 hours. After culture, the developing genitalia were examined for changes in GT outgrowth and morphology, using *Hoxa13*^{GFP} expression as a marker of the relevant tissues.

Dihydroxytestosterone (DHT; Sigma) was dissolved in 100% ethanol and diluted to 10 nM in BgJb media. GT explants were grown for 6 hours in the presence of 10 nM DHT or the equivalent carrier volume of ethanol. After culture, the explants were fixed in 4% paraformaldehyde and processed for in situ hybridization using the *Shh* or *Hoxa13* riboprobes as described above.

Antibody blocking

E12.5 genital tubercles were dissected from *Hoxa13*^{GFP} heterozygous mutant embryos and grown for 72 hours in the BTC rotary culture apparatus. Culture media consisted of BGJb media (Sigma-Aldrich) buffered with 10 mM HEPES and supplemented with 0.1 mg/ml ascorbic acid. The sealed culture bottles were continuously supplied with humidified gas containing 40% O_2, 5% CO_2 and 55% N_2. Polyclonal antibodies specific for *Bmp4* (*αBmp4*) or *Bmp7* (*αBmp7*; R and D Systems) were added to the media at a concentration of 4 μg/ml, whereas control cultures were treated with 2 μg/ml of whole-goat immunoglobulins (IgGs). After 36 hours, 50% of the culture media was replaced with new aliquots of antibody or control IgGs. After 72 hours, the genital tubercles were examined for changes in meatus formation, as well as defects in urethral groove closure using *Hoxa13*^{GFP} expression as a marker. To assess changes in PCD in response to antibody blocking, GT explants from E12.5 *Hoxa13*^{GFP}-heterozygous embryos were grown, using the same rotary culture conditions, for 24 hours in media containing 4 μg/ml *αBmp7* or control IgGs. After culture, the explants were fixed in 4% paraformaldehyde and assessed for changes in programmed cell death by TUNEL analysis of frozen sections as described.

RESULTS

Hoxa13-deficient mice exhibit reduced mitosis in the genital tubercle

As hypospadia predominantly affects the development and closure of the urethra and its meatus, we first examined whether mice lacking *Hoxa13* exhibited any changes in mitosis or programmed cell death that could contribute to the hypospadiac phenotype. Examination of the *Hoxa13*^{GFP} allele (this work) (Stadler et al., 2001) indicates that the GFP expression patterns recapitulate previously reported patterns of *Hoxa13* expression in mouse and other vertebrate species (Warot et al., 1997; Haack and Gruss, 1993; Yokouchi et al., 1991). In the GT, *Hoxa13*^{GFP} expression is detected in the surrounding mesenchyme as well as the UPE, a structure previously identified as an essential signaling center for GT outgrowth (Fig. 1A,B) (Perriton et al., 2002; Haraguchi et al., 2000; Haraguchi et al., 2001; de Santa Barbara et al., 2002). Examination of the GT at E12.5 revealed no major differences in the early formation of the UPE or mesenchymal shelves,

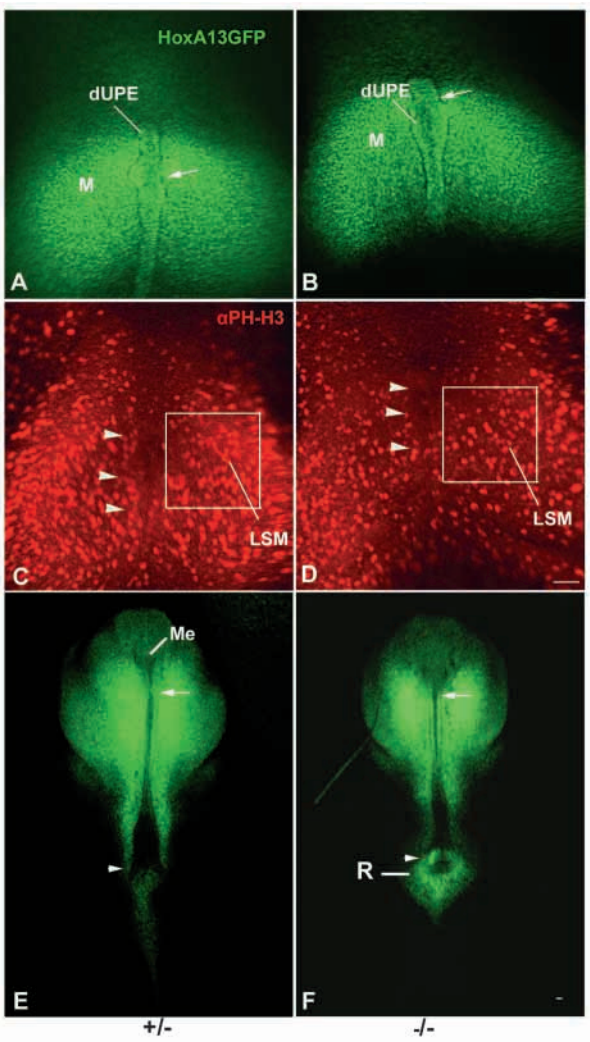

Fig. 1. Characterization of hypospadiac and proliferative defects in Hoxa13^{GFP}-homozygous mutants. (A,B) *Hoxa13*^{GFP} is expressed in both the GT mesenchyme (M) as well as the urethral plate epithelium (UPE) in E12.5 littermates. Arrows denote the distal UPE (dUPE) which is thickened in homozygous mutants. (C,D) Proliferation in the GT mesenchyme of E12.5 male embryos. Proliferation was measured in the lateral shelf mesenchyme (LSM) by counting phosphohistone H3 positive cells in a 2.5×2.5 cm region (white square). Note that proliferation is maintained in the cells immediately adjacent to the UPE in heterozygous embryos (C, arrowheads), whereas mutant embryos exhibit a dramatic decrease immediately adjacent to the UPE (D, arrowheads). (E) Closure of the distal urethra and glans by proliferating mesenchyme in an E15.5 heterozygous male embryo. Arrow denotes the initial site of closure. Arrowhead indicates future site of the rectal mesenchyme condensation. (F) Hypospadia in homozygous-mutant littermates. Arrow denotes the loss of urethral closure as well as the persistence of the epidermal layer, which is not covered by the proliferating mesenchyme. Arrowhead indicates precocious condensation of rectal mesenchyme. Note that formation of the rectum (R) is precocious and more rostral in homozygous mutants (F). Scale bars: 50 μm.

with the exception that the distal UPE in homozygous mutants was consistently thicker (Fig. 1A,B). Analysis of cell proliferation in the GT also revealed distinct differences between homozygous-mutant and heterozygous-mutant embryos. In particular, homozygous mutants consistently demonstrated less proliferation in the mesenchyme flanking the proximal UPE (Fig. 1C; arrowheads), as well as in the lateral shelf tissues, which exhibited 46% (±6%) fewer mitotic cells when compared with controls (Fig. 1C,D; boxed regions). Interestingly, little proliferation could be detected in the UPE (Fig. 1C,D) for any genotype examined. To determine the impact of reduced mesenchymal shelf proliferation on urethral growth and closure, we examined the formation and closure of the distal urethra and meatus. In male embryos, differentiation of external genitalia begins at approximately E14.5 with growth of the glans penis and formation of the urethral meatus proceeding from the distal portion of the GT (Kaufman and Bard, 1999; Murakami, 1987). In E15.5 heterozygotes, the urethral groove epithelium was less visible because of the progression of the surrounding mesenchyme (Fig. 1E). In the distal urethra, fusion of the urethral folds was clearly visible, establishing the site of the urethral meatus (Fig. 1E). In homozygous mutants, the urethral groove remained exposed, with no fusion of the distal mesenchyme leaving the placement and formation of the distal meatus undefined (Fig. 1F).

In the caudal GT, *Hoxa13* also regulates the formation of the rectum. In the heterozygous controls, rectal development proceeds from a centralized core of epithelium (Fig. 1E; arrowhead) flanked by mesenchyme expressing *Hoxa13*^{GFP}. In homozygous mutants, both the placement and maturation of the rectal epithelium is affected, resulting in the formation of a more ventralized rectum one gestational day earlier (Fig. 1F).

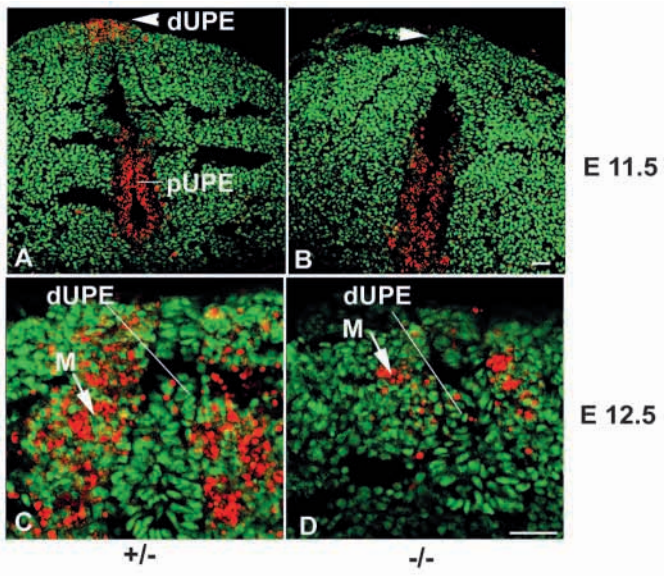

Fig. 2. Male embryos lacking Hoxa13 exhibit decreased programmed cell death (PCD) in the developing genital tubercle. (A) At E11.5, PCD is restricted to the dUPE (arrowhead) and proximal UPE (pUPE) in heterozygous controls. (B) PCD is reduced in the dUPE (arrowhead), but not in the pUPE of *Hoxa13*^{GFP}-homozygous mutants. (C) By E12.5, PCD shifts from the dUPE to the mesenchyme (M) flanking the dUPE (arrow). (D) Homozygous mutants also exhibit a shift in PCD to the flanking mesenchyme, although the number of TUNEL-positive cells in the mutant mesenchyme is consistently reduced when compared with heterozygous controls. Scale bars: 50 μm.

Hoxa13 mutants exhibit reduced programmed cell death in the differentiating male GT

During GT development, programmed cell death (PCD) precedes the crucial fusion events necessary for the growth and closure of the penile urethra (Haraguchi et al., 2001; van der Werff et al., 2000). To determine if changes in PCD also contribute to the hypospadiac phenotype, apoptosis in the developing GT was measured using a TUNEL assay. By E11.5, PCD was readily seen in the distal and proximal UPE of wild-type (not shown) and heterozygous *Hoxa13*^{GFP}-mutant embryos (Fig. 2A). By contrast, homozygous mutants consistently exhibited reduced PCD in the distal UPE, whereas the proximal UPE showed no difference in PCD when compared with controls (Fig. 2A,B). Quantitation of PCD in the distal UPE of homozygous mutants revealed, on average, a 90% (±8%) loss in TUNEL-positive cells when compared with controls (Fig. 2A,B).

By E12.5, both homozygous mutant and control embryos exhibited a shift in PCD from the UPE to the surrounding mesenchyme (Fig. 2C,D). A comparison of PCD levels in the mesenchymal tissue revealed an 85% (±5%) reduction in PCD in homozygous mutants (Fig. 2C,D) when compared with heterozygous controls. TUNEL-positive cells were no longer detectable in the UPE or surrounding mesenchyme by E14.5 in both homozygous-mutant and control embryos (data not shown).

The expression of Bmp7 and Nog are affected in Hoxa13^{GFP} mutants

To address mechanisms underlying reduced PCD in the mutant GT, we first determined the localization and timing of pro-apoptotic signals in this region. In particular, the expression of *Bmp4* and *Bmp7* was examined, as these factors regulate many of the apoptotic events necessary for normal limb (Macias et al., 1997), craniofacial (Graham et al., 1996) and inner ear (Fekete et. al., 1997) development. Although no differences in *Bmp4* expression could be discerned between homozygous-mutant and control embryos (data not shown), notable changes in *Bmp7* expression were seen in the UPE and lateral shelf mesenchyme (Fig. 3). At E12.5, wild-type embryos exhibited high levels of *Bmp7* expression along the entire axis of the UPE, as well as in more proximal lateral shelf mesenchyme (Fig. 3A). By contrast, mutant embryos express *Bmp7* only in distal UPE, with little expression seen in the lateral shelf mesenchyme (Fig. 3B). Mutant embryos also exhibit a thickened layer of epithelium (Fig. 3B) that physically separates the growing glans from the more ventral UPE.

By E14.5, *Bmp7* expression was highest in the distal glans at the site of meatus formation, as well as in the urethral epithelium that is covered with a thin layer of mesenchyme and in the developing preputial glands (Fig. 3C). In homozygous mutants, *Bmp7* expression was noticeably reduced in the distal glans, whereas no expression could be detected in the urethral epithelium that lacked a covering layer of mesenchyme in all embryos examined (4/4; Fig. 3D).

We next examined whether homozygous-mutant embryos

exhibited any changes in the expression of Bmp antagonists or Bmp-target genes that would augment reduced *Bmp7* expression in the GT and contribute to the hypospadiac phenotype. In E11.5 wild-type embryos, *Nog* expression was strongest in the lateral shelf mesenchyme, with no expression in the UPE or mesenchyme adjacent to the UPE (Fig. 3E).

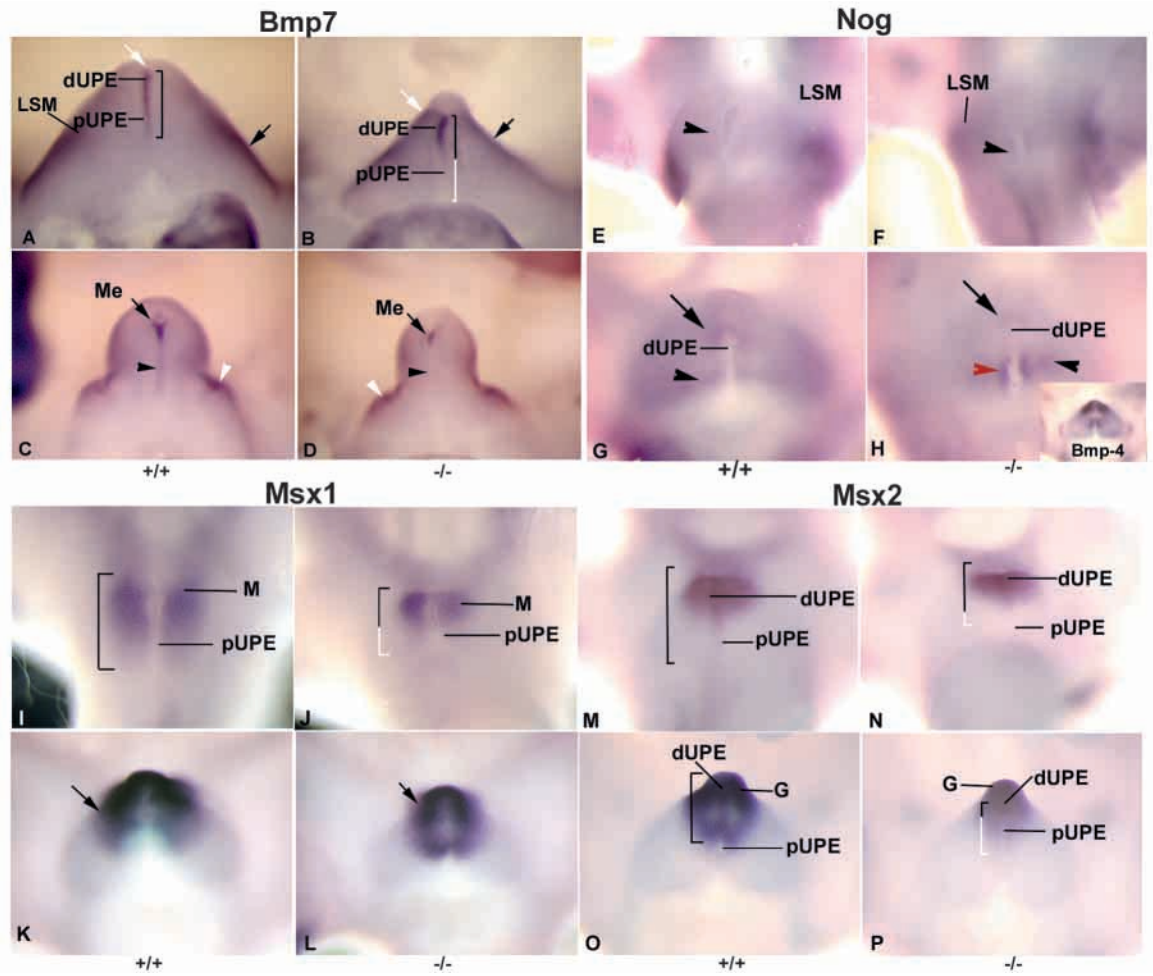

Fig. 3. The expression of *Bmp7*, its target genes, *Msx1* and *Msx2*, and its antagonist, *Nog*, are affected in Hoxa13^{GFP}-mutant embryos. (A) Expression of *Bmp7* in the UPE and lateral shelf mesenchyme (LSM; black arrow) in E12.5 control embryos. Black bracket shows sites of gene expression, white portion of brackets show sites where gene expression is absent. White arrow denotes the thin layer of epidermis. (B) Absence of *Bmp7* expression in pUPE of E12.5 male homozygous mutants, as well as in the later shelf mesenchyme (black arrow). Note the thickened epithelial layer (white arrow) in the distal genital tubercle. (C) Expression of *Bmp7* in E14.5 male wild-type embryos. Note high levels of *Bmp7* expression in the developing meatus (black arrow), as well as in the urethral epithelium which is covered by mesenchyme (black arrowhead) and the developing preputial gland (white arrowhead). (D) Malformation of the meatus is concomitant with reduced *Bmp7* expression in E14.5 male homozygous mutants (black arrow). Note that *Bmp7* expression is reduced in the preputial gland (white arrowhead) and absent in the epithelial chord (black arrowhead), which is not covered by mesenchyme. (E) *Nog* is normally expressed in the lateral shelf mesenchyme (LSM) of E11.5 wild-type embryos. Black arrowhead in E denotes position of ectopic *Nog* expression seen in the mesenchyme flanking pUPE in E11.5 male homozygous mutants (F). (G) In E12.5 control embryos, *Nog* is expressed at low levels in mesenchyme flanking the pUPE (black arrowhead); dUPE (black arrow). (H) E12.5 homozygous mutants exhibit strong ectopic *Nog* expression in the mesenchyme adjacent to the medial-proximal UPE (red arrowhead), as well as in a narrow band in the GT mesenchyme (black arrowhead). *Nog* expression was reduced in the mesenchyme flanking the dUPE in these same mutant embryos (black arrow). Inset (H) reflects *Bmp4* expression in the mesenchyme flanking the medial-proximal UPE. (I) In E11.5 wild-type embryos, *Msx1* expression is localized to the mesenchyme (M) flanking the entire UPE. Black bracket marks the rostral-caudal extent of *Msx1* expression. (J) In E11.5 homozygous mutants, *Msx1* expression is absent in the mesenchyme flanking the pUPE. Black portion of bracket represents *Msx1* expression in the rostral mesenchyme. White portion of bracket represents caudal portion of mesenchyme lacking *Msx1* expression. (K) In E12.5 embryos, *Msx1* is predominantly expressed in the distal GT where the glans will eventually form (black arrow); in homozygous mutants (L) this is noticeably reduced in size (black arrow). (M) *Msx2* is strongly expressed in the rostral mesenchyme, as well as in the UPE and sinus epithelium in E11.5 wild-type male embryos. Black bracket denotes *Msx2* expression along the rostral-caudal axis of the genital tubercle. (N) Homozygous mutants also exhibit strong *Msx2* expression in the UPE and mesenchyme flanking the dUPE (black portion of bracket); however, no expression could be detected in pUPE as denoted by the white portion of the bracket. (O) In E12.5 embryos, *Msx2* is expressed in the developing glans mesenchyme (G) as well as in the UPE. Black bracket reflects continuous UPE expression of *Msx2*. (P) In E12.5 mutants, *Msx2* expression is also seen in the dUPE (black portion of bracket) and glans (G), whereas no *Msx2* expression is seen in the dUPE (white portion of the bracket).

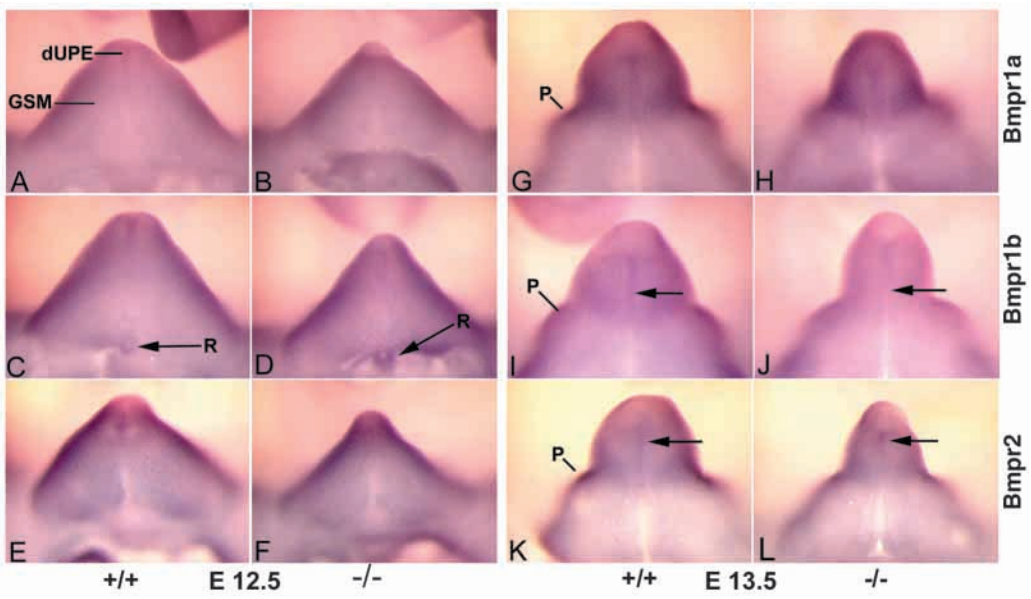

Fig. 4. Bmp-receptor expression is affected in Hoxa13^{GFP}-homozygous mutants. (A,B) Low levels of *Bmpr1a* can be detected in both wild-type and mutant E12.5 embryos in the dUPE and GSM. (C,D) *Bmpr1b* expression is elevated in developing rectum (R) (black arrows) of homozygous mutant E12.5 embryos. (E,F) *Bmpr2* expression is present in the UPE and GSM of both wild-type and mutant E12.5 embryos. (G,H) In E13.5 embryos, *Bmpr1a* expression is restricted to the distal genital tubercle and the developing preputial glands (P) in both wild-type and homozygous mutants. (I,J) *Bmpr1b* expression is reduced in the UPE (arrows) of E13.5 homozygous mutants when compared with wild type controls. (K,L) *Bmpr2* expression appears elevated in the UPE of E13.5 homozygous mutants (arrows), whereas expression in the developing preputial glands (P) appears unaffected.

By contrast, homozygous mutants exhibited ectopic *Nog* expression in the mesenchyme immediately flanking the proximal UPE (Fig. 3F). By E12.5, *Nog* expression was most noticeable in the lateral shelf mesenchyme and mesenchyme flanking the distal UPE (Fig. 3G). In homozygous mutants, ectopic *Nog* expression was most visible in the mesenchyme adjacent to the medial and proximal UPE (Fig. 3H), a region that overlaps with the normal expression pattern of *Bmp4* (Fig. 3H; inset). A second Bmp antagonist, gremlin, exhibited no changes in GT expression between mutant and wild-type embryos (data not shown).

Next we examined whether reduced *Bmp7* expression as well as ectopic *Nog* expression in the GT were sufficient to affect the expression of the Bmp-target genes *Msx1* and *Msx2*. In E11.5 wild-type embryos, *Msx1* expression was highest in the mesenchyme immediately adjacent to the proximal UPE (Fig. 3I). In homozygous mutants, *Msx1* expression was greatly reduced in the mesenchymal tissues flanking the proximal UPE (Fig. 3J). By E12.5, *Msx1* expression is restricted to the distal glans region (Fig. 3K), which is smaller in the mutant male embryo (Fig. 3L).

Interestingly, *Msx2* expression is seen throughout the UPE, as well as in the mesenchyme flanking the distal UPE of E11.5 wild-type embryos (Fig. 3M). In homozygous mutants, *Msx2* expression is absent in the proximal UPE in the same region as *Bmp7* expression is reduced (Fig. 3B) and adjacent to the site of ectopic *Nog* expression (Fig. 3H). In the rostral GT, *Msx2* expression appears normal, which is consistent with the levels of *Bmp7* expression in this region (Fig. 3N). By E12.5, *Msx2* expression is highest in the developing glans and throughout the UPE (Fig. 3O), whereas in homozygous mutants, no *Msx2* expression could be seen in the more proximal UPE (Fig. 3P). The lack of *Msx2* expression in the proximal UPE is consistent with the loss of *Bmp7* expression in the proximal UPE of *Hoxa13*^{GFP}-homozygous mutants (Fig. 3B,D).

Bmp-receptor expression is altered in Hoxa13^{GFP}-mutant embryos

We next examined the expression of Bmp-receptors *Bmpr1a, Bmpr1b,* and *Bmpr2* in GT of *Hoxa13*^{GFP} embryos. At E12.5, all three receptors are uniformly expressed at low levels throughout the genital shelf mesenchyme (GSM) and UPE of wild-type male embryos (Fig. 4A,C,E). However, in *Hoxa13*^{GFP}-homozygous mutants, elevated levels of *Bmpr1b* expression was consistently seen in the condensing rectal mesenchyme (compare Fig. 4C and D). At E 13.5, Bmp-receptor expression was confined to the developing glans, UPE and preputial gland condensations in wild type and homozygous mutants (Fig. 4G-L). Interestingly, in homozygous mutants, *Bmpr1b* expression was reduced in the mid-proximal UPE (Fig. 4; compare I and J), whereas *Bmpr2* expression appeared elevated in the distal UPE when compared with controls (Fig. 4K,L).

Perturbations in Bmp signaling recapitulate defects caused by loss of Hoxa13 function in the external genitalia

To correlate changes in Bmp signaling with the defects associated with loss of *Hoxa13* function, we examined whether blocking Bmp signaling during GT outgrowth could recapitulate the homozygous-mutant phenotype in unaffected *Hoxa13*^{GFP}-heterozygous embryos. Blocking antibodies specific for Bmp4 (*αBmp4*) or Bmp7 (*αBmp7*) were applied to cultured GTs from E12.5 *Hoxa13*^{GFP} heterozygous male embryos. In control experiments, GT explants treated with whole-serum immunoglobulins (IgGs) exhibited normal development of the urethra and glans, which after 72 hours were similar in size and morphology to the external genitalia of E15.5 male embryos (Fig. 1). In the developing glans and urethra, treatments with control IgGs had no affect on the formation of a meatus (M) or the progression of the mesenchyme necessary for urethral closure in 4 out of 5

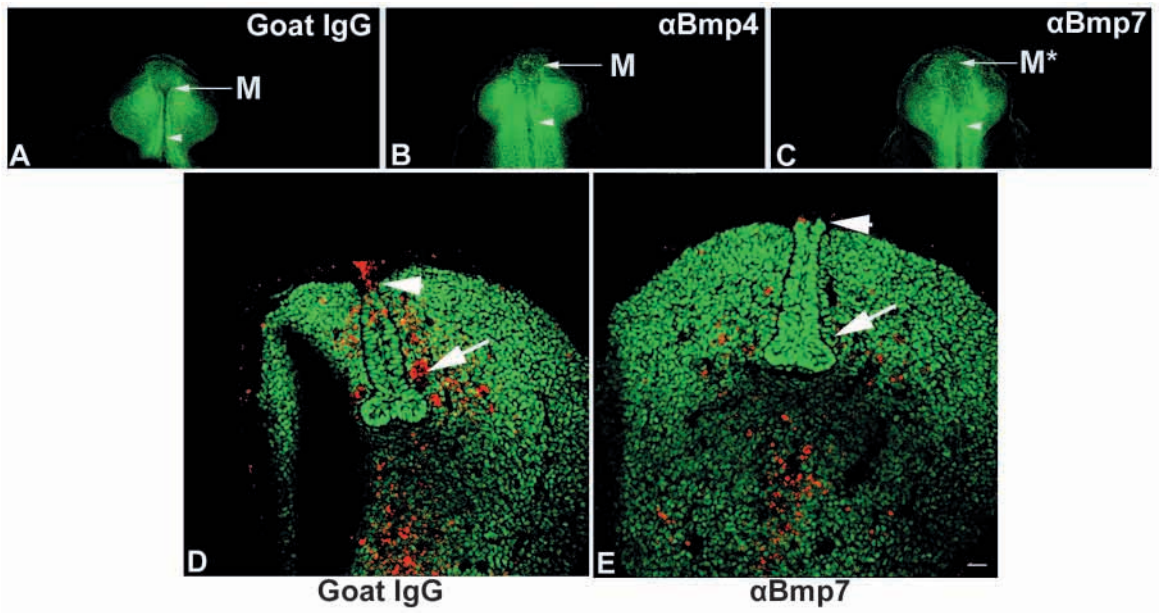

Fig. 5. Blocking of Bmp7 and Bmp4 signaling recapitulates the Hoxa13^{GFP} homozygous mutant phenotype. (A) Heterozygous male GT explant treated with control IgGs. Arrow denotes the normal formation of the meatus (M), arrowhead denotes the progression of mesenchyme closing the urethra. (B) Male GT explant treated with a *Bmp4*-blocking antibody (αBmp4). Arrow denotes the disruption of meatus (M) formation. Arrowhead denotes the formation of an ectopic fistula. (C) Male GT explant treated with a *Bmp7*-blocking antibody (αBmp7**)**. Arrow denotes the complete absence of a meatus (M*). Arrowhead denotes poor progression of the GT mesenchyme to close the urethra. (D) TUNEL analysis of PCD in the UPE of heterozygous male GT explants treated with control IgGs. Arrowhead denotes normal levels of PCD in the dUPE. Arrow denotes normal levels of PCD in the mesenchyme flanking the UPE. (E) TUNEL analysis of PCD of a male GT explant treated with the *Bmp7*-blocking antibody (αBmp7**)**. Note the reduced PCD in the dUPE **(**arrowhead) and mesenchyme flanking the UPE (arrow) when compared with the IgG-treated control. Scale bar: 50 μm.

embryos tested (Fig. 5A). Next, although *Bmp4* expression was unaffected in the GT *Hoxa13*^{GFP} homozygous mutants, we hypothesized that its function in the GT may be antagonized by the ectopic expression of *Nog* in the mesenchyme flanking the UPE (Fig. 3F,H), a site that highly expresses *Bmp4* (Fig. 3H; inset). To test this hypothesis, *Hoxa13*^{GFP}-heterozygous explants were treated with *αBmp4*. After 72 hours, dramatic changes in the growth and closure of the urethra were observed, which caused either partial (3/8) or complete ablation (5/8) of the developing meatus, as well as affecting the progression of urethral mesenchyme, causing a fistula in the sub-glans region in all embryos (8/8) examined (Fig. 5B). Similarly, explants treated with *αBmp7* also exhibited partial (2/5) or complete (3/5) ablation of the meatus, as well as defects in glans morphology, which appeared rounded in all (5/5) treated explants (Fig. 5C). A comparison of the GT phenotypes elicited by *αBmp7* and *αBmp4* treatments with the malformations exhibited by *Hoxa13*^{GFP}-homozygous mutants (Fig. 1F) reveal a high degree of similarity, particularly in meatus where loss of *Hoxa13* function causes either partial or complete ablation of the meatus in all homozygous-mutant embryos examined (Fig. 1F).

Explants treated with *αBmp7* also exhibited a thickening of the epithelial plate (Fig. 5C), a phenotype detected by E12.5 and persisting to E15.5 in *Hoxa13*^{GFP} homozygous male mutants (Fig. 1B,F). Interestingly, the effects on meatus development elicited by *αBmp4* and *αBmp7* treatments were identical in female GT explants (data not shown), which suggests that the signals required for meatus cavitation function prior to the sex-specific differentiation of these tissues. Finally, we examined whether the blocking of *Bmp7* signals could also reproduce changes in PCD seen in the UPE and GT mesenchyme of *Hoxa13*^{GFP}-homozygous mutants (Fig. 2). Indeed, heterozygous GT explants treated with *αBmp7* for 24 hours exhibited dramatic reductions in PCD in the distal UPE and adjacent mesenchyme when compared with heterozygous explants treated with control IgGs (Fig. 5D,E). These results confirm that PCD in the GT mesenchyme requires *Bmp7* signaling, which is reduced in the UPE of *Hoxa13*^{GFP}-homozygous mutants.

GT proliferation defects result from reduced Fgf8 signaling and can be rescued in vitro by Fgf8 supplementation

As Fgf8 produced by the UPE directs many of the proliferative events during GT development (Haraguchi et al., 2000), we examined whether loss of *Hoxa13* function affects *Fgf8* expression and signaling in this region. In the GT, *Fgf8* expression was highest at E11.5 in both wild type and homozygous mutants (Fig. 6A,B). Section analysis of Fgf8 expression in the UPE revealed marked differences in the localization of Fgf8 transcripts between wild-type and homozygous mutant embryos. Specifically, wild-type embryos express Fgf8 throughout the UPE, providing a proliferative signal along the entire GT axis (Fig. 6C). By contrast, *Hoxa13*^{GFP}-homozygous mutants exhibit a dramatic reduction of *Fgf8* expression in the proximal UPE, whereas expression in the distal UPE appears unaffected (Fig. 6D). Interestingly, the genital shelf mesenchyme immediately adjacent to the proximal UPE is also the site of poor proliferation in E11.5

embryos lacking *Hoxa13* (Fig. 6; compare I,J with K,L), which suggests that reduced Fgf8 expression in this region causes this defect in proliferation.

To test whether the loss of *Fgf8* expression in the proximal UPE of homozygous-mutant embryos is sufficient to account for reduced proliferation in genital shelf mesenchyme, heparin acrylic beads soaked in BSA or Fgf8b were placed in the proximal UPE of homozygous mutant GT explants. In all cases (4/4), Fgf8b-treated beads rescued the proliferation defects seen in the surrounding mesenchyme (Fig. 6K,L), restoring mitotic levels throughout the GT (Fig. 6H). Identical treatments using BSA-treated beads caused no change in the proliferative defect (Fig. 6G), which closely resembled the levels of proliferation exhibited by E11.5 homozygous-mutant embryos (Fig. 6K). Extended culture of E11.5 mutant GTs for 3 days in the presence of Fgf8b had no discernable effect on urethra or meatus development when compared with BSA-treated controls (data not shown). This suggests that *Fgf8* expression in the UPE provides mainly the initial proliferative impetus to the surrounding mesenchyme.

Stratification and signaling defects in the UPE are independent of sonic hedgehog function in the developing GT

To determine if the loss of *Fgf8* expression in the proximal UPE reflects a change in the polarization of the UPE, we examined the expression of *Shh* in the GT of E12.5 *Hoxa13*^{GFP} embryos. Analysis of *Shh* expression in the UPE showed no differences in expression between wild-type and homozygous-mutant embryos (Fig. 7A,B), which confirms that polarizing signals are normally produced in the mutant UPE. The presence of *Shh* expression in the mutant proximal UPE strongly suggests that *Hoxa13* is required for *Fgf8* expression in the proximal UPE, as a more generalized effect would have also affected *Shh* expression in this region.

Section analysis of the UPE of E12.5 embryos revealed distinct differences in epithelial cell morphology, stratification and cytokeratin expression patterns. In particular, epithelial cells in the wild-type (not shown) and heterozygous UPE appeared more mature, as defined by their cuboidal shape, stratification and expression of cytokeratin (K) 14 (K-14) (Fig. 7A,C). By contrast, the cells within the mutant UPE appeared less mature, as defined by their rounded morphology, poor stratification and reduced K-14 expression (Fig. 7B,D). Finally, the expression of K-8 and K-18 in these same tissues (Fig. 7E,F) confirms that reduced K-14 expression in the epithelia of homozygous mutants is specific for this maturation marker and is not a result of a generalized loss in epithelial cell identity, as K-8/18 are typically expressed in most simple epithelia (Kuzrock et al., 1999).

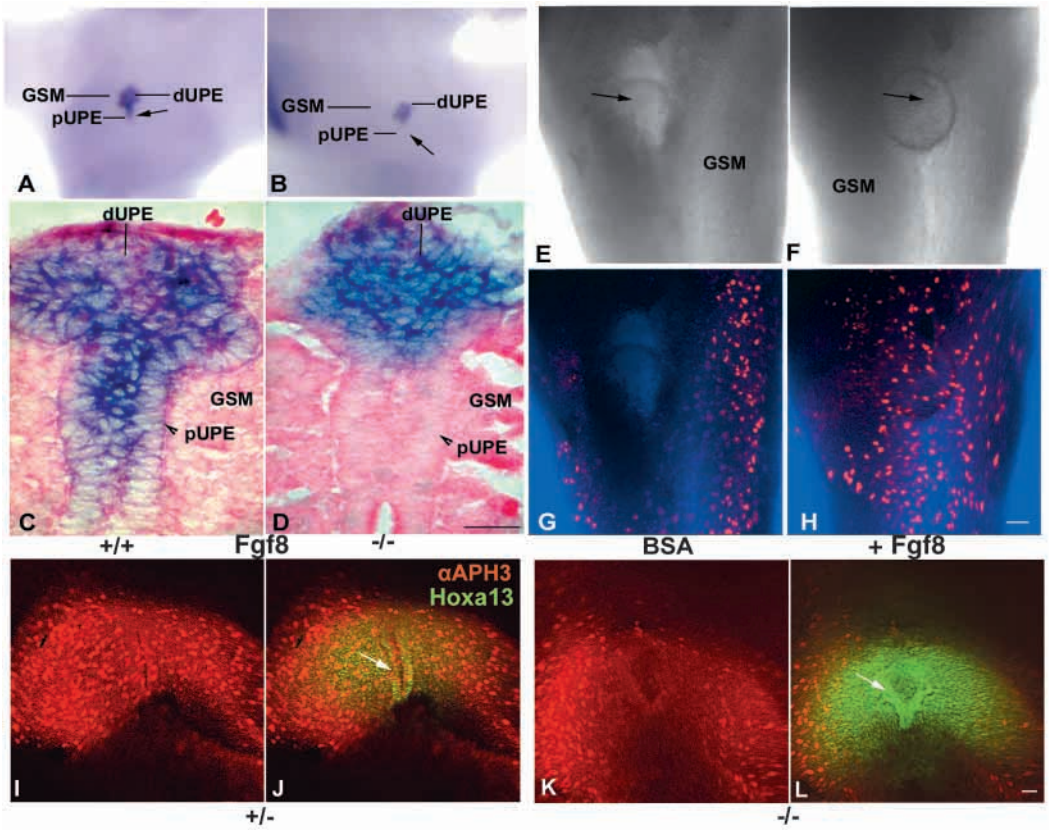

Fig. 6. Ectopic application of Fgf8 rescues reduced GT proliferation in Hoxa13^{GFP}-homozygous mutants. (A) Expression of Fgf8 in the genital tubercle of E11.5 wild-type male embryos. Note that Fgf8 expression is seen in both dUPE and pUPE (black arrow) of E11.5 wild-type male embryos. Genital Shelf Mesenchyme, GSM. (B) Fgf8 expression is absent in the pUPE (arrow) of E 11.5 *Hoxa13*^{GFP}-homozygous mutants. (C) Section analysis of Fgf8 expression in the urethral plate epithelium (UPE) of E11.5 wild type male embryos. Note that Fgf8 expression is present in both the proximal (arrowhead) and distal UPE. (D) Fgf8 expression is restricted to the dUPE in E11.5 homozygous mutants. Note the complete loss of Fgf8 expression in the pUPE (arrowhead). (E,G) Implantation of heparin beads (arrow) treated with BSA into the UPE of E11.5 homozygous mutants had no effect on the reduced proliferation seen in the GSM. (F,H) Implantation of beads treated with 0.1 mg/ml Fgf8b (arrow) stimulated proliferation of the GSM in age-matched homozygous mutant embryos. (I,J) Typical levels of cell proliferation in the E11.5 GT of normally developing heterozygous male embryos. Arrow denotes normal thickening of the UPE. (K,L) Cell proliferation in the GT of a E11.5 *Hoxa13*^{GFP} homozygous male mutant. Arrow denotes the earliest detection of the abnormally thickened UPE. Note how Fgf8 applications alter cell proliferation in the mutant GT to resemble proliferation levels exhibited by heterozygous littermates (compare H with I), whereas mutant embryos treated with BSA maintain reduced levels of cell proliferation (compare G with K). Scale bars: 50 μm.

Embryos lacking Hoxa13 exhibit aberrant vascular development in distal GT

Next, because changes in Tgfβ signaling can also affect tissue vascularization, we examined whether changes in the expression of the Tgfβ family member *Bmp7* and its antagonist, *Nog*, might also affect GT vascularization. Section analysis of the distal urethra and glans revealed dramatic differences between heterozygous- and homozygous-mutant embryos in the vascularization of these tissues. In E13.5 heterozygous and wild-type (not shown) embryos, the mesenchyme immediately flanking the UPE is vascularized by fine capillary vessels 10-15 μm in diameter (Fig. 8A). By contrast, the same region in homozygous mutants was consistently (10/10) vascularized by vessels typically ranging from 70-150 μm in diameter (Fig. 8B). Cellular analysis of these enlarged vessels confirmed them to be functional vascular tissue, containing an endothelium expressing the angiogenic marker Pecam-1 (CD31; Pecam – Mouse Genome Informatics) (Fig. 8A,B) as well as red blood cells (Fig. 7B). Interestingly, vessel endothelial cells of heterozygous embryos strongly co-express Pecam and Hoxa13^{GFP} as determined the yellow co-localized signal (Fig. 8A), whereas in homozygous mutants the degree of Pecam and Hoxa13^{GFP} co-localization was greatly reduced in the endothelial cells (Fig. 8B).

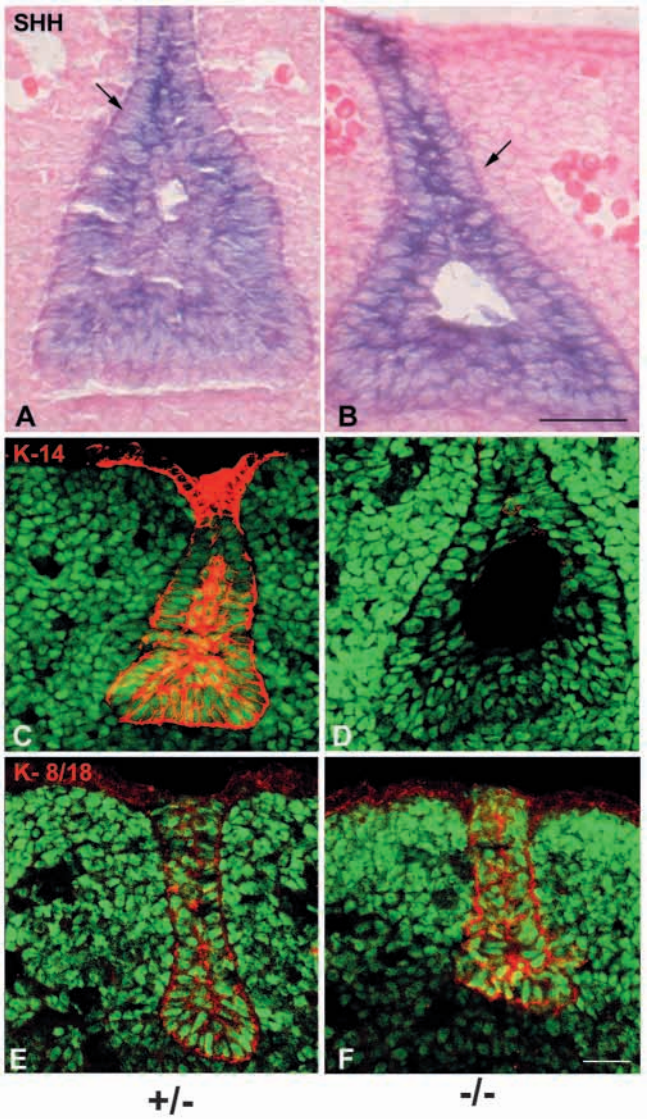

Fig. 7. Stratification and differential cytokeratin expression in the UPE and sinus epithelium in E12.5 Hoxa13^{GFP} male embryos. (A,B) Sonic hedgehog (Shh) expression in the UPE is unaffected by loss of *Hoxa13* function. Arrows denote a shift in epithelial morphology and stratification from a multilayered cuboidal shape (A) to rounded simple epithelium (B) in homozygous mutants. (C) Cytokeratin 14 (K-14) is highly expressed in the stratified epithelium of heterozygous embryos. (D) K-14 expression is severely reduced in the UPE of *Hoxa13*^{GFP}-homozygous mutants, whereas both control and homozygous-mutant embryos exhibit normal levels of cytokeratin 8/18 expression in the same epithelial tissues (E,F). Scale bars: 50 μm.

Section analysis of the distal GT at E13.5 also provided a possible explanation for distal closure defects seen in Fig. 1F, where the protrusion of the UPE throughout the distal urethra places a physical barrier of epithelium at the site where progressing mesenchymal shelves meet and fuse (Fig. 8B). By contrast, the UPE in heterozygous littermates was consistently regressed below the level of the progressing mesenchyme, providing a clear path for the progressing mesenchyme to join and fuse (Fig. 8A).

Androgen signaling is reduced in Hoxa13-deficient embryos

To characterize the relationship between *Hoxa13* and the androgen signals necessary for GT growth and development, we examined the expression of the androgen receptor (AR) in the developing glans and urethra of E15.5 littermates. In the distal urethra of heterozygous embryos, AR proteins are detected in the surface ectoderm as well as in the condensing mesenchyme proximal and lateral to the urethral epithelium (Fig. 9A). In homozygous mutants, AR expression is reduced in the surface ectoderm as well as in the mesenchyme proximal and lateral to the hypospadiac urethral epithelium (Fig. 9B). Interestingly the medial mesenchymal condensation (Fig. 9A,C,D) reflects the anlagen from which the penian bone (P) develops postnatally, under the control of androgen signaling (Murakami, 1987). In *Hoxa13*^{GFP}-homozygous mutants, this condensation is absent in the more distal sections of the penis (Fig. 9B), and appears disorganized in more proximal sections when compared with heterozygous controls (Fig. 9C,D). This lack of mesenchymal condensation is remarkably similar to the phenotype exhibited in the autopod of *Hoxa13*^{GFP}-mutant mice (Stadler et al., 2001), which suggests a similar role for *Hoxa13* in regulating mesenchymal cell adhesion and provides an explanation for hypoplasia of the os-penis in Hypodactyly mice (Post and Innis, 1999).

In more proximal sections, AR expression co-localizes with Hoxa13^{GFP} in the penial mesenchymal condensation and in the lateral mesenchyme flanking the urethral epithelium (Fig. 9C). By contrast, homozygous mutants exhibit little AR expression in the lateral mesenchyme adjacent the urethral epithelium, although strong AR-Hoxa13^{GFP} co-localization is detected in an ectopic region approximately 50-80 μm from the urethral epithelium (Fig. 9D). Finally, we evaluated whether *Hoxa13* could also be regulated by the AR ligand, dihydroxytestosterone (DHT). DHT treatments of cultured genital tubercles (10 nM) from wild-type or homozygous-

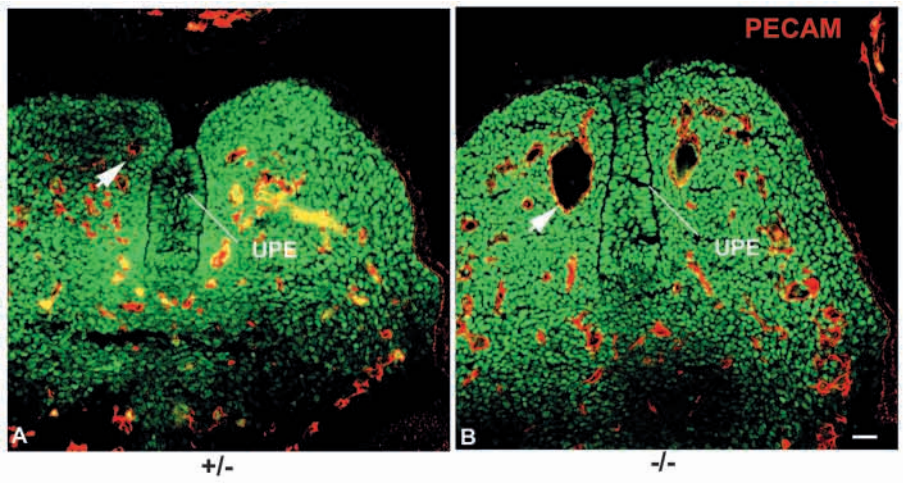

Fig. 8. Capillary vessel malformations in the genital tubercle of Hoxa13 deficient embryos. (A) Capillary vessel localization detected by the vascular endothelial marker CD-31 (Pecam; red) in E13.5 heterozygous male embryos. Note the strong co-localization of *Hoxa13*^{GFP}(green) with the Pecam-positive capillary endothelial cells (yellow), as well as the symmetric arrangement of capillary vessels around the UPE (arrowhead). (B) Expansion of the capillary vessels in the E13.5 homozygous mutant genital tubercle. Arrowhead denotes a typical sevenfold expansion in vessel diameter in the mutant genital tubercle. Note the lack of *Hoxa13*^{GFP} co-localization (yellow) with Pecam in the capillary vessels in the mutant GT. Scale bar: 50 μm.

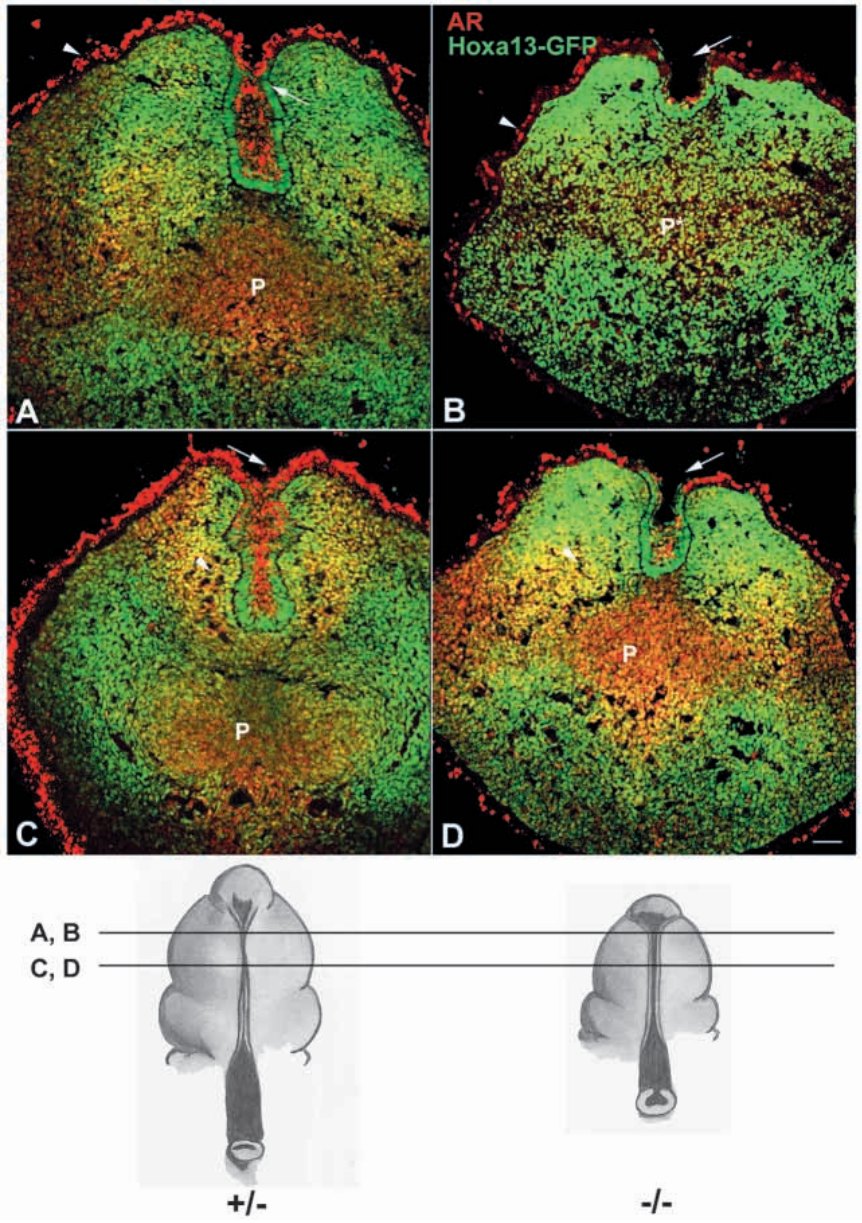

Fig. 9. Androgen receptor (AR) expression in the developing glans and penile urethra of E15.5 Hoxa13^{GFP} male embryos. (A) AR expression is elevated in the UPE (arrow) as well as the surface ectoderm (arrowhead) of heterozygous controls. In these same embryos, the penian bone condensation (P) is readily detected. (B) AR expression in the distal glans of a homozygous mutant. Arrow denotes hypospadiac UPE. Arrowhead denotes reduced AR expression in the surface ectoderm. Note the poor condensation of the penian bone mesenchyme (P*). (C) A more proximal cross-section through the glans. Arrowhead denotes high levels of Hoxa13^{GFP}/AR co-localization (yellow cells) in the mesenchyme immediately adjacent the UPE. Arrow denotes high levels of AR expression in the glans ectoderm. Note the extensive condensation of mesenchyme forming the penian bone (P). (D) Hoxa13^{GFP}/AR co-localization (yellow cells) is absent from the mesenchyme flanking the UPE in homozygous mutants and is relocated to the lateral glans mesenchyme (arrowhead). Arrow denotes reduced AR expression in the ectoderm covering the UPE. AR expression was also seen in the penian bone condensation (P), which was more disorganized than was the same site in the heterozygous control. Scale bar: 50 μm. (Below) Diagram to show planes of section through the developing glans and penile urethra (lines A,B and C,D).

mutant male embryos (E13.5) showed no elevation in *Hoxa13* expression relative to ethanol treated controls (data not shown).

DISCUSSION

In this study, we present evidence that hypospadia in mice lacking *Hoxa13* is caused by defects in UPE maturation, signaling and proliferative induction of the surrounding genital tubercle mesenchyme. Recently, studies by Haraguchi et al. (Haraguchi et al., 2000; Haraguchi et al., 2001) and Perriton et al. (Perriton et al., 2002) indicate that the UPE functions as a signaling center, secreting Shh and Fgf8, which are necessary for GT outgrowth and closure. To date, the unique functions of these factors during GT formation have been difficult to discern as mice lacking Shh fail to form a defined UPE from which Fgf8 is produced (Haraguchi et al., 2001). Our analysis of GT development in *Hoxa13*^{GFP}-homozygous mutants separates the individual function(s) of *Shh* and *Fgf8*, as well as identifies *Bmp7* as a third UPE signaling molecule whose function is essential for the development and closure of the meatus and urethra.

In a model of *Hoxa13* function during GT development (Fig. 10A,B,D), we conclude that *Hoxa13* is required for the normal expression of *Fgf8* and *Bmp7* in the UPE, as well as the repression of *Nog* in the mesenchyme flanking the UPE. In the absence of *Hoxa13* function (Fig. 10C,E), defects in the external genitalia can be attributed to perturbations in three essential processes. First, reduced Fgf8 signaling from the proximal UPE causes a dramatic decrease in the initial proliferation of the GT mesenchyme, a process previously shown to be essential for the development of the external genitalia (Haraguchi et al., 2000; Perriton et al., 2002). Second, reduced *Bmp7* signaling lowers the amount of Msx1 and Msx2 expression in the mesenchyme flanking the proximal UPE, causing a decrease in PCD necessary for the removal of overlying ectoderm, urethral tube closure and meatus formation. Finally, *Hoxa13* is required for the repression of *Nog* in the mesenchyme flanking the medial-proximal UPE, a site where *Bmp4* signaling has an essential role in mediating urethral tube closure. Surprisingly, we did not see an elevation in PCD in the distal urethra and glans, which are noticeably smaller in *Hoxa13*^{GFP} homozygous mutants. This finding is consistent with the normal levels of Shh expression in the UPE of *Hoxa13*^{GFP} mutants, which was previously shown to confer cell survival in tissues derived from the hindgut or foregut endoderm (Perriton et al., 2002; Litingtung et al., 1998). By this same mechanism, elevated levels of Shh in the UPE of *Hoxa13*^{GFP}-homozygous mutants could contribute to the reduced PCD seen in these tissues, although we see no evidence for elevated *Shh* expression in the UPE of *Hoxa13*^{GFP} homozygous mutant embryos.

Clearly, the signals emanating from the UPE are complex, as both proliferative (Fgf8) and pro-apoptotic (Bmp7) signals impact the developing GT in overlapping temporal and spatial domains. What is intriguing about this signaling is how the GT mesenchyme interprets the appositional roles of *Fgf8* and *Bmp7* to regulate the growth and closure of the external genitalia. In *Hoxa13*^{GFP}-mutant mice, small changes in these appositional signals, manifest as either coronal or

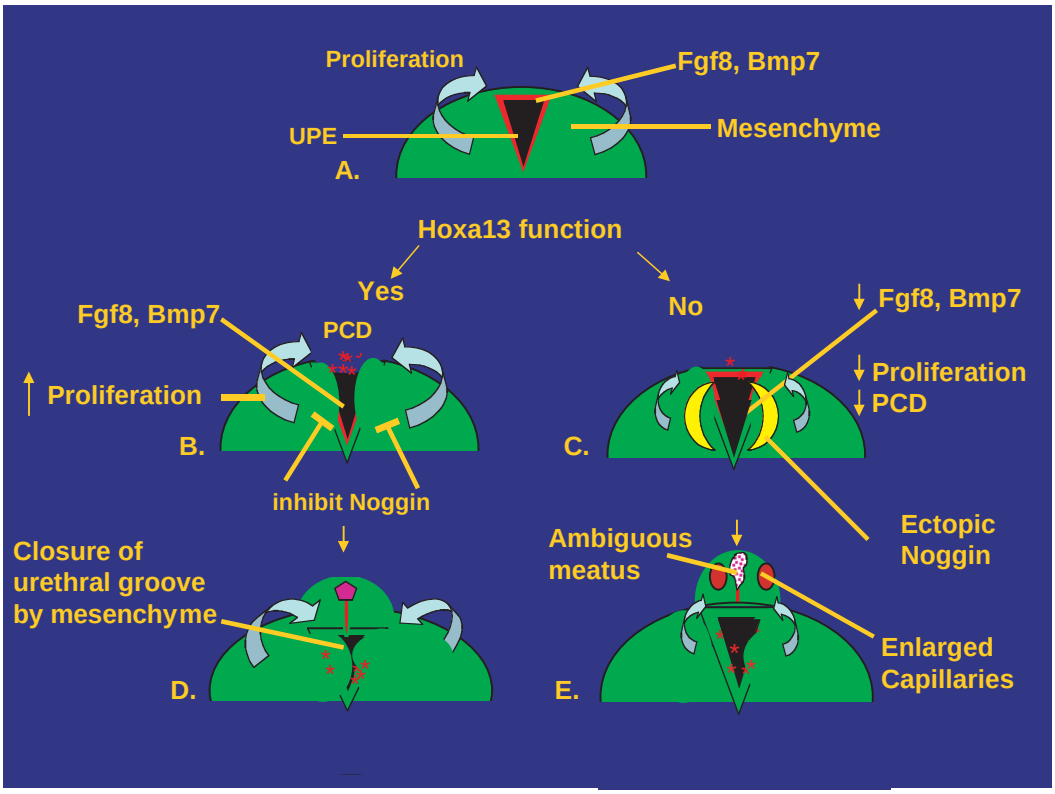

Fig. 10. A model for Hoxa13 function during development of the external genitalia. (A) *Fgf8* and *Bmp7* are co-expressed in the UPE at E11.5, whereas *Hoxa13*^{GFP} is expressed in the UPE as well as the GT mesenchyme. (B,D) *Hoxa13* is essential for normal expression of *Fgf8* and *Bmp7* in the UPE, as well as for the mesenchymal repression of *Nog*. In combination, these signals control cell proliferation and PCD to establish normal formation of the meatus and urethral tube closure. (C,E) In the absence of *Hoxa13* function, *Fgf8* and *Bmp7* expression is reduced in the UPE, whereas *Nog* expression is ectopic, which, in combination, causes decreased cell proliferation, reduced PCD and capillary vessel enlargement, as well as defects in urethral tube closure and meatus development. Asterisks indicate sites of programmed cell deaths. Red triangle in A indicates regions of colocalized *Fgf8*, *Bmp7* and *Hoxa13* expression. The developing meatus in D is indicated by the purple symbol.

coronal/urethral hypospadia. Recognizing the sensitivity of the developing GT to changes in Bmp and Fgf signaling, it is possible that perturbations in these same signaling events contribute to the rising incidence in hypospadias affecting the human birth population (Paulozzi et al., 1997). Warranting close scrutiny would be the role of environmental factors in perturbing signaling between *Fgf8*, *Bmp7* or *Bmp4* and their receptors during GT development.

Similarly, because no changes in *Fgf10* or *Wnt7a* expression could be detected in GT of *Hoxa13*^{GFP} mutants (data not shown), it is likely that *Bmp7*, *Bmp4* and *Fgf8* function as the predominant factors required for GT outgrowth. This conclusion is supported by the rescue of GT proliferation by ectopic Fgf8 application (this work) (Haraguchi et al., 2000), as well as studies in chick where the overexpression of truncated *Hoxa13* proteins caused reduced *Fgf8* expression and severe malformations of the gut and genitourinary regions (de Santa Barbara and Roberts, 2002). Recently, studies of β-catenin function in the developing limb (Barrow et al., 2003) also revealed a role for this molecule in mediating GT outgrowth, as mice lacking β-catenin in the GT exhibit hypoplasia of the GT and its derivatives (J. Barrow, personal communication).

Failure to stratify the UPE contributes to the hypospadiac phenotype

By E12.5 the UPE exhibits changes in cell morphology and cytokeratin expression that are indicative of maturation and stratification of the epithelial signaling center. In particular, cells lining the UPE shift from a layer of simple epithelium to several cuboidal cell layers (stratified) that now express K-14, a cytokeratin that is normally found in differentiating epithelium (Kuzrock et al., 1999; Kivela and Uusitalo, 1998; Coulombe and Omary, 2002). In homozygous-mutant littermates, stratification and K-14 expression are compromised, resulting in the disorganized arrangement of rounded cells in the UPE. This phenotype may be attributed to the focal loss of K-14 expression in the UPE, as mice lacking K-14 exhibit defects in the stratification of the skin and corneal epithelium (Lloyd et al., 1995). Interestingly, the loss of epithelial keratins is often associated with elevated PCD (McGowan et al., 2002; Oshima, 2002). However, in proximal UPE of *Hoxa13*^{GFP}-homozygous mutants no significant changes in PCD were observed. This result is explained by the maintenance of K-8/18 expression in mutant UPE, which protects epithelium from PCD by directly binding pro-apoptotic proteins, including the Tradd domain of Tnf receptor 1, as well as providing structural support to minimize PCD initiated by mechanical stress (Inada et al., 2001; Marceau et al., 2001; Baribault et al., 1993; Baribault et al., 1994). Similarly, changes in the stratification and keratin expression patterns in the UPE could also affect cell-cell interactions between the progressing mesenchyme and the underlying epithelium, preventing the efficient movement of mesenchymal cells necessary for urethral closure.

PCD as a mechanism to remove the distal UPE and its secreted factors

An examination of PCD during GT development suggests a highly dynamic interplay between mesenchymal proliferation and apoptosis. Using a TUNEL assay, PCD was first detected in the cloacal membrane (CM) covering the GT (data not shown). Within 12 hours, a rapid shift in PCD had occurred, moving from CM ectoderm to the endodermal tissues of the UPE. What is intriguing about this shift in PCD is its coincidence with peak Fgf8 expression in the UPE. Developmentally, the localization of PCD in the UPE could serve two important functions. First, the removal of the UPE by PCD could modulate levels of *Fgf8* expression, providing a signal for differentiation to occur; a similar use of PCD is seen in the developing limb, where removal of the AER reduces *Fgf8* signaling to stimulate differentiation of the underlying mesenchyme (Zwilling, 1955; Saunders et al., 1957; Macias et al., 1997; Niswander et al., 1994). Second, to achieve closure of the urethra, the progressing mesenchyme must cover the medial epithelial layer. In *Hoxa13*^{GFP}-homozygous mutants, the epithelial layer is elevated and thickened, which would inhibit closure of the medial urethral by the proliferating mesenchyme. After UPE removal, PCD shifts again to the mesenchymal tissues immediately flanking the UPE, occurring as early as E12.5 and persisting in the mesenchyme until closure of the penile urethra (Baskin et al., 2001; van der Werff et al., 2000). Mechanistically, the reduction of PCD in the urethral mesenchyme of *Hoxa13*^{GFP}-mutant mice helps to explain the pathology of the hypospadiac phenotype, where the persistence of thickened urethral epithelium places a physical barrier between the progressing mesenchymal shelves.

Bmp signaling and GT development

Our analysis of GT development in the presence of Bmp4 and Bmp7 blocking antibodies strongly suggests a role for these factors in mediating growth and closure of the meatus and urethra. Here, an analysis of GT development in embryos lacking either *Bmp7* or *Bmp4*, or combinations of both, would provide the most corroborative data to define the complete function of these molecules during the formation of the external genitalia. To date, no characterizations of *Bmp7* function in the external genitalia have been reported, although *Bmp7* has been shown to play an essential role in mediating kidney tubule formation, as well as in the production of meiotic germ cells (Luo et al., 1995; Dudley et al., 1995; Dudley and Robertson, 1997; Zhao et al., 2001). Similarly, the function of *Bmp4* in the developing GT is unknown as embryos lacking *Bmp4* die between E6.5 and E9.5 (Winnier et al., 1995). Recognizing the similarity in phenotypes between blocked Bmp signaling and those exhibited by *Hoxa13*^{GFP}-homozygous mutants, it is probable that the defects in meatus formation and urethral tube closure seen in *Hoxa13*^{GFP}-mutant mice reflect the combined effects of reduced *Bmp7* expression and those elicited by *Nog* antagonism.

Hoxa13 is essential for maintaining capillary vessel diameter and morphology

Normally, vascularization of the developing glans is provided by two well-defined rings of capillary beds supplying both the prepuce and the mesenchyme immediately adjacent the UPE. In *Hoxa13*^{GFP} mutants, capillary vessel morphology, placement and diameter are dramatically altered in the distal glans. Interestingly, this phenotype is also present in the glans clitoris of homozygous mutant female mice (data not shown), reflecting the common origin of these two structures and conservation of the mechanisms underlying this gross change

in vessel diameter. Aberrant vascularization of the glans is also associated with human hypospadias, and was interpreted as a default state stemming from the aborted differentiation of the glans, meatus and urethral spongiosum (Baskin et al., 1998; Baskin, 2000). Clearly the enlargement of the capillary vessels in the glans of *Hoxa13*^{GFP} homozygous mutant mice reflects more than a default vascular state as only the distal vessels supplying the glans are affected, whereas the entire glans and urethra are hypoplastic in these mice.

Mechanistically, changes in Tgfβ or Smad signaling also affect blood vessel development, morphology and diameter (reviewed by Dennler et al., 2002; ten Dijke et al., 2002; Weinstein et al., 2000; Oh et al., 2000; Vargesson and Laufer, 2001). In particular, mice lacking Smad5 (Madh5 – Mouse Genome Informatics) exhibit many of the same defects shown by *Bmp4*- and *Tgf-beta 1*- (*Tgfb1* – Mouse Genome Informatics) null mice, including enlarged blood vessels (Yang et al., 1999; Chang et al., 1999). Our examination of *Bmp4* and *Bmp7* function in the developing GT indicates that although *Bmp7* is uniquely expressed in the UPE, both molecules function similarly in the glans to regulate the formation of the meatus. Here the combinatorial effects of perturbed *Bmp4* and *Bmp7* signaling may contribute the enlargement of the glans capillary vessels. We cannot exclude the possibility that changes in Bmp-receptor expression in the developing glans, could also contribute to the enlarged capillary vessel phenotype, although the expression of receptors Bmpr1a, Bmpr1b and Bmpr2 in the glans was not significantly different between E13.5 homozygous-mutant and control embryos.

Hoxa13 is required for normal androgen receptor expression in the developing GT

Our examination of AR localization in the developing murine GT revealed a high degree of co-localization between *Hoxa13* and the AR in the proximal urethral mesenchyme. By contrast, only minor levels of AR protein could be detected in the same mesenchymal regions of *Hoxa13*^{GFP}-homozygous mutants. This reduction in AR expression appears specific to the mesenchyme immediately adjacent to the urethral epithelium, and suggests a role for *Hoxa13* in mediating the responsiveness of these tissues to androgens by modulating the levels of AR in the urethral epithelium. This modulation in AR expression would provide a developmental link between hypospadias associated with environmental antagonists of the AR and hypospadias associated with loss of *Hoxa13* function, placing *Hoxa13* as an important modulator of AR signaling during the development of the external genitalia (Baatrup and Junge, 2001; Curtis, 2001; Baskin et al., 2001). Alternatively, environmental compounds could affect *Hoxa13* expression directly, in a manner similar to the ectopic expression of Hox genes in response to exogenous retinoids (Simeone et al., 1991; Whiting, 1997).

In mice, the prenatal response of the GT to AR signaling is the growth and closure of urethra and glans penis, as mice lacking AR signaling also exhibit hypospadia (Murakami, 1987). Postnatally, AR signaling is required for the formation of the os-penis (Murakami, 1987). Here, the function of *Hoxa13* in mediating the postnatal development of the external genitalia is unknown as *Hoxa13* mutations derived from homologous recombination are not compatible with life beyond E15.5 (Stadler et al., 2001; Fromental-Ramain et al., 1996). An examination of os-penis formation in hypodactyly mice (Post and Innis, 1999) suggests that *Hoxa13* mediates similar mesenchymal condensation events as described in the limb (Stadler et al., 2001). However, it is important to note that the hypodactyly mutation in *Hoxa13* also affects the expression of *Hoxd13* causing phenotypes more similar to those of *Hoxa13*/*Hoxd13*-compound mutants (Robertson et al., 1996; Robertson et al., 1997; Fromental-Ramian, 1996).

Using conditional mutagenesis, *Hoxa13* function could be completely assessed throughout genitourinary development. This analysis would provide important clues regarding the developmental pathology underlying hypospadias beyond E15.5 while also providing an important resource to examine both neonatal development and adult maintenance of genitourinary tissues affected by loss of *Hoxa13* function.

The authors wish to thank Gen Yamada, Nancy Manley and Alan Godwin for the critical reading of this manuscript. We would also like to thank Mario Capecchi for allowing our continued investigation of phenotypes in the Hoxa13^{GFP}-knockout mouse. This work was supported by grants to H.S.S. from the National Institutes of Health/NIDDK (5R01DK5915-01) and the March of Dimes Birth Defects Foundation (Basil O'Connor Starter Scholar Research Award Grant number 5-FY00-521).

REFERENCES

Allera, A., Herbst, M. A., Griffin, J. E., Wilson, J. D., Schweikert, H. U. and McPhaul, M. J. (1995). Mutations in the androgen receptor coding sequence are infrequent in patients with isolated hypospadias. *J. Clin. Endocrinol. Metab.* **80**, 2697-2699.

Baatrup, E. and Junge, M. (2001). Antiandrogenic pesticides disrupt sexual characteristics in the adult male guppy. *Environ. Health Perspect.* **109**, 1063-1070.

Baribault, H., Price, J., Miyai, K. and Oshima, R. G. (1993). Mid-gestational lethality in mice lacking keratin 8. *Genes Dev.* **7**, 1191-1202.

Baribault, H., Penner, J., Iozzo, R. V. and Wilson-Heiner, M. (1994). Colorectal hyperplasia and inflammation in keratin 8 knockout mice. *Genes Dev.* **8**, 2964-2973.

Barrow, J. R., Thomas, K. R., Boussadia-Zahui, O., Moore, R., Kemler, R., Capecchi, M. R. and McMahon, A. P. (2003). Ectodermal Wnt3/beta-catenin signaling is required for the establishment and maintenance of the apical ectodermal ridge. *Genes Dev.* **17**, 394-409.

Baskin, L. S. (2000). Hypospadias and urethral development. *J. Urol.* **163**, 951-956.

Baskin, L. S., Erol, A., Li, Y., Wu, Y. and Cunha, G. R. (1998). Anatomical studies of hypospadias. *J. Urol.* **160**, 1108-1115.

Baskin, L. S., Erol, A., Jegatheesan, P., Li, Y., Liu, W. and Cunha, G. R. (2001). Urethral seam formation and hypospadias. *Cell Tissue Res.* **305**, 379-387.

Chang, H., Huylebroeck, D., Verschueren, K., Guo, Q., Matzuk, M. M. and Zwijsen, A. (1999). Smad5 knockout mice die at mid-gestation due to multiple embryonic and extraembryonic defects. *Development* **126**, 1631-1642.

Coulombe, P. A. and Omary, M. B. (2002). Hard and soft principles defining the structure and function and regulation of keratin intermediate filaments. *Curr. Opin. Cell Biol.* **14**, 110-122.

Cunha, G. R. (1972). Tissue interactions between epithelium and mesenchyme of the urogenital and integumental origin. *Anat. Rec.* **172**, 529-541.

Cunha, G. R. and Lung, B. (1978). The possible influence of temporal factors in androgenic responsiveness of urogenital tissue recombinants from wild-type and androgen-insensitive (Tfm) mice. *J. Exp. Zool.* **205**, 181-193.

Curtis, L. R. (2001). Organophosphate antagonism of the androgen receptor. *Toxicol. Sci.* **60**, 1-2.

Dennler, S., Goumans, M. J. and ten Dijke, P. (2002). Transforming growth factor beta signal transduction. *J. Leukoc. Biol.* **71**, 731-740.

de Santa Barbara, P. and Roberts, D. J. (2002). Tail gut endoderm and

gut/genitourinary/tail development: new tissue-specific role for *Hoxa13*. *Development* **129**, 551-561.

Dudley, A. T., Lyons, K. M. and Robertson, E. J. (1995). A requirement for bone morphogenic protein-7 during development of the mammalian kidney and eye. *Genes Dev.* **9**, 2795-2807.

Dudley, A. T. and Robertson, E. J. (1997). Overlapping expression of bone morphogenetic protein family members potentially account for limited tissue defects in Bmp7 deficient embryos. *Dev. Dyn.* **208**, 349-362.

Fekete, D. M., Homburger, S. A., Waring, M. T., Riedl, A. E. and Garcia, L. F. (1997). Involvement of programmed cell death in morphogenesis of the vertebrate inner ear. *Development* **124**, 2451-2461.

Fromental-Ramain, C., Warot, X., Messadecq, N., LeMeur, M., Dollé, P. and Chambon, P. (1996). Hoxa-13 and Hoxd-13 play a crucial role in the patterning of the limb autopod. *Development* **122**, 2997-3011.

Gallentine, M. L., Morey, A. F. and Thompson, I. M., Jr (2001). Hypospadias: a contemporary epidemiologic assessment. *Pediatr. Urol.* **57**, 788-790.

Giedion, A. and Prader, A. (1976). Hand-foot-uterus (HFU) syndrome with hypospadias: the hand-foot-genital (HFG) syndrome. *Pediatr. Radiol.* **4**, 96-102.

Goodman, F. R., Bacchelli, C., Brady, A. F., Brueton, L. A., Fryns, J. P., Mortlock, D. P., Innis, J. W., Holmes, L. B., Donnenfeld, A. E., Feingold, M. et al. (2000). Novel *HOXA13* mutations and the phenotypic spectrum of hand-foot-genital syndrome. *Am. J. Hum. Genet.* **67**, 197-202.

Graham, A., Koentges, G. and Lumsden, A. (1996). Neural crest apoptosis and the establishment of craniofacial pattern: an honorable death. *Mol. Cell. Neurosci.* **8**, 76-83.

Haack, H. P. and Gruss, P. (1993). The establishment of murine Hox-1 expression domains during patterning of the limb. *Dev. Biol.* **157**, 410-422.

Haraguchi, R., Suzuki, K., Murakami, R., Sakai, M., Kamikawa, M., Kengaku, M., Sekine, K., Kawano, H., Kato., S., Ueno, N. and Yamada, G. (2000). Molecular analysis of external genitalia formation: the role of fibroblast growth factor (Fgf) genes during genital tubercle formation. *Development* **127**, 2471-2479.

Haraguchi, R., Mo, R., Hui, C., Motoyama, J., Makino, S., Shiroishi, T., Gaffield, W. and Yamada, G. (2001). Unique functions of Sonic hedgehog during external genitalia development. *Development* **128**, 4241-4250.

Inada, H., Izhawa, I., Nishizawa, M., Fujita, E., Kiyono, T., Takahashi, T., Momoi, T. and Inagski, M. (2001). Keratin attenuates tumor necrosis factor-induced cytotoxicity through associated with TRADD. *J. Cell Biol.* **155**, 415-426.

Kaufman, M. H. and Bard, J. B. L. (1999). The urogenital system. In *The Anatomical Basis of Mouse Development*, pp. 109-132. New York: Academic Press.

Kivela, T. and Uusitalo, M. (1998). Structure, development, and function of cytoskeletal elements in non-neuronal cells of the human eye. *Prog. Retinal Eye Res.* **17**, 385-428.

Kuzrock, E. A., Baskin, L. S., Li, Y. and Cunha, G. R. (1999). Epithelial-mesenchymal interactions in the development of the mouse fetal genital tubercle. *Cell Tissues Organs* **164**, 125-130.

Litingtung, Y., Lei, L., Westphal, H. and Chiang, C. (1998). Sonic hedgehog is essential to foregut development. *Nat. Genet.* **20**, 58-61.

Lloyd, C., Yu, Q. C., Cheng, J., Turksen, K., Degenstein, L., Hutton, E. and Fuchs, E. (1995). The basal keratin network of stratified squamous epithelia: defining K15 function in the absence of K14. *J. Cell Biol.* **129**, 1329-1344.

Luo, G., Hofmann, C., Brockers, A. L., Sohocki, M., Bradley, A. and Karsenty, G. (1995). *Bmp-7* is an inducer of nephrogenesis, and is also required for eye development and skeletal patterning. *Genes Dev.* **9**, 2808-2820.

Macias, D., Ganan, Y., Sampath, T. K., Piedra, M. E., Ros, M. A. and Hurle, J. M. (1997). Role of Bmp-2 and OP-1 (*BMP-7*) in programmed cell death and skeletogenesis during chick limb development. *Development* **124**, 1109-1117.

Manley, N. R. and Capecchi, M. R. (1995). The role of Hoxa-3 in mouse thymus and thyroid development. *Development* **121**, 1989-2003.

Marceau, N., Loranger, A., Gilbert, S., Daigle, N. and Champetier, S. (2001). Keratin-mediated resistance to stress and apoptosis in simple epithelial cells in relation to health and disease. *Biochem. Cell Biol.* **79**, 543-555.

McGowan, K. M., Tong, X., Colucci-Guyon, E., Langa, F., Babinet, C. and Coulombe, P. A. (2002). Keratin 17 null mice exhibit age- and strain-dependent alopecia. *Genes Dev.* **16**, 1412-1422.

Mortlock, D. P. and Innis, J. W. (1997). Mutation of *HOXA13* in hand-foot-genital syndrome. *Nat. Genet.* **156**, 179-180.

Murakami, R. (1987). A histological study of the development of the penis of wild-type and androgen-insensitive mice. *J. Anat.* **153**, 223-231.

Murakami, R. and Mizuno, T. (1986). Proximal-distal sequence of development of the skeletal tissues in the penis of rat and the inductive effect of epithelium. *J. Embryol Exp. Morph.* **92**, 133-143.

Niswander, L. S., Jeffrey, S., Martin, G. R. and Tickle, C. (1994). A positive feedback loop coordinates growth and patterning of the vertebrate limb. *Nature* **371**, 609-612.

Oh, S. P., Seki, T., Goss, K. A., Imamura, T., Yi, Y., Donahoe, P. K., Li, L., Miyazono, K., ten Dijke, P., Kim, S. and Li, E. (2000). Activin receptor like kinase 1 modulates transforming growth factor beta 1 signaling in the regulation of angiogenesis. *Proc. Natl. Acad. Sci. USA* **97**, 2626-2631.

Oshima, R. G. (2002). Apoptosis and keratin intermediate filaments. *Cell Death Differ.* **9**, 486-492.

Paulozzi, L. J., Erickson, D. and Jackson, R. J. (1997). Hypospadias trends in two US surveillance systems. *Pediatrics* **100**, 831-834.

Perriton, C. L., Powles, N., Chiang, C., Maconochie, M. K. and Cohn, M. J. (2002). Sonic hedgehog signaling from the urethral plate epithelium controls external genitalia development. *Dev. Biol.* **247**, 26-46.

Podlasek, C. A., Duboule, D. and Bushman, W. A. (1997). Male accessory sex organ morphogenesis is altered by loss of function of Hoxd-13. *Dev. Dyn.* **208**, 1-12.

Podlasek, C. A., Barnett, D. H., Clemens, Q., Bak, P. M. and Bushman, W. (1999). Prostate development requires Sonic Hedgehog expressed by the urogenital sinus epithelium. *Dev. Biol.* **209**, 28-39.

Post, L. C. and Innis, J. W. (1999). Infertility in adult hypodactyly mice is associated with hypospadia of distal reproductive structures. *Biol. Reprod.* **61**, 1402-1408.

Poznanski, A. K., Kuhns, L. R., Lapides, J. and Stern, A. M. (1975). A new family with the hand-foot-genital syndrome – a wider spectrum of the hand-foot-uterus syndrome. *Birth Defects Orig. Artic. Ser.* **11**, 127-135.

Roberston, K. E., Chapman, M. H., Adams, A., Tickle, C. and Darling, S. M. (1996). Cellular analysis of limb development in the mouse mutant hypodactyly. *Dev. Genet.* **19**, 9-25.

Robertson, K. E., Tickle, C. and Darling, S. M. (1997). Shh, Fgf4, and Hoxd gene expression in the mouse limb mutant hypodactyly. *Int. J. Dev. Biol.* **41**, 733-736.

Saunders, J. W., Jr, Cairns, J. M. and Gasseling, M. T. (1957). The role of the apical ridge of ectoderm in the differentiation of the morphological structure and inductive specificity of limb parts of the chick. *J. Morphol.* **101**, 57-88.

Silver, R. and Russel, D. (1999). 5a reductase type 2 mutations are present in some boys with isolated hypospadias. *J. Urol.* **162**, 1142-1145.

Simeone, A., Acampora, D., Nigro, V., Faiella, A., D'Esposito, M., Stornaiuolo, A., Mavilio, F. and Boncinelli, E. (1991). Differential regulation by retinoic acid of the homeobox genes for the four HOX loci in human embryomal carcinoma cells. *Mech. Dev.* **33**, 215-227.

Stadler, H. S., Higgins, K. M. and Capecchi, M. R. (2001). Loss of Eph-receptor expression correlates with loss of cell adhesion and chondrogenic capacity in *Hoxa13* mutant limbs. *Development* **128**, 4177-4188.

Stern, A. M., Gall, J. C., Jr, Perry, B. L., Stimson, C. W., Weitkamp, L. R. and Poznanski, A. K. (1970). The hand-foot-uterus syndrome: a new hereditary disorder characterized by hand and foot dysplasia, dermatoglyphic, abnormalities, and partial duplication of the female genital tract. *J. Pediatr.* **77**, 109-116.

Sutherland, R. W., Wiener, J. S., Hicks, J. P., Marcelli, M., Gonzales, E. T., Jr, Roth, D. R. and Lamb, D. J. (1996). Androgen receptor gene mutations are rarely associated with isolated penile hypospadias. *J. Urol.* **156**, 828-831.

ten Dijke, P., Goumans, M. J., Itoh, F. and Itoh, S. (2002). Regulation of cell proliferation by Smad proteins. *Cell Physiol.* **191**, 1-16.

van der Hoeven, F., Zánkány, J. and Duboule, D. (1996a). Gene transpositions in the HoxD complex reveal a hierarchy of regulatory controls. *Cell* **85**, 1025-1035.

van der Hoeven, F., Sordino, P., Fraudeau, N., Izpisua-Belmonte, J. C. and Duboule, D. (1996b). Teleost HoxD and HoxA genes: comparison with tetrapods and functional evolution of the HOXD complex. *Mech. Dev.* **54**, 9-21.

van der Werff, J. F., Nievelstein, R. A., Brands, E., Luijsterburg, A. J. and

Vermeij-Keers, C. (2000). Normal development of the male anterior urethra. *Teratology* **61**, 172-183.

Vargesson, N. and Laufer, E. (2001). Smad7 misexpression during embryonic angiogenesis causes vascular dilation and malformations independently of vascular smooth muscle function. *Dev. Biol.* **15**, 499-516.

Warot, X., Fromental-Ramain, C., Fraulob, V., Chambon, P. and Dollé, P. (1997). Gene dosage-dependent effects of Hoxa-13 and hoxd-13 mutations on morphogenesis of the terminal parts of the digestive system and urogenital tracts. *Development* **124**, 4781-4791.

Weinstein, M., Yang, X. and Deng, C. (2000). Functions of mammalian Smad genes as revealed by targeted gene disruption in mice. *Cytokine Growth Factor Rev.* **11**, 49-58.

Whiting, J. (1997). Craniofacial abnormalities induced by the ectopic expression of homeobox genes. *Mutat. Res.* **396**, 97-112.

Winnier, G., Blsessing, M., Labosky, P. A. and Hogan, B. L. (1995). Bone morphogenic protein-4 is required for mesoderm formation and patterning in the mouse. *Genes Dev.* **9**, 2105-2116.

Yang, X., Castilla, L. H., Xu, X., Li, C., Gotay, J., Weinstein, M., Liu, P. P. and Deng, C. X. (1999). Angiogenesis defects and mesenchymal apoptosis in mice lacking SMAD5. *Development* **126**, 1571-1580.

Yokouchi, Y., Sasaki, H. and Kuroiwa, A. (1991). Homeobox gene expression correlated with bifurcation process of limb cartilage development. *Nature* **353**, 443-445.

Zhao, G. Q., Chen, Y. X., Liu, X. M., Xu, Z. and Qi, X. (2001). Mutation in Bmp7 exacerbates the phenotype of Bmp8a mutants in spermatogenesis and epididymis. *Dev. Biol.* **240**, 212-222.

Zhao, Y. and Potter, S. S. (2001). Functional specificity of the *Hoxa13* homeobox. *Development* **128**, 3197-3207.

Zwilling, E. (1955). Ectoderm-mesoderm relationship in the development of the chick embryo limb bud. *J. Exp. Zool.* **128**, 423-441.